Original Article

Auto-delineation of the hippocampus using Mask R-CNN for radiation oncology: A cross-sectional observational study

Adwait Laud, Kaustav Talapatra[1], Manoj Sankhe[2], Ajinkya Gupte[3], Ashish Shetty[2], Nikhil Bardeskar[4], Prashasti Kanikar, Abhishek Rout[2], Shubhangi Barsing[3], Pranjal Tiwari, Arya Shah, Deepak Patkar[5]

Department of Computer Engineering NMIMS University, MPSTME, [1]Department of Radiation Oncology Nanavati Max Super Speciality Hospital, [2]Department of Electronics and Telecommunications NMIMS University, MPSTME, [5]Director, Medical Services and Head, Department of Radiology and Imaging, [3]Department of Radiation Oncology Nanavati Max Super Speciality Hospital, [4]Nanavati Max Institute of Cancer Care, Nanavati Max Super Speciality Hospital, Mumbai, Maharashtra, India

For correspondence: Dr. Kaustav Talapatra, Nanavati Max Super Speciality Hospital, Mumbai - 400 056, Maharashtra, India. E-mail: kaustee@gmail.com

Submitted: 14-Jul-2023
Revised: 24-Aug-2023
Accepted: 18-Sep-2023
Published: 20-Dec-2024

Access this article online
Website: https://journals.lww.com/cancerjournal
DOI: 10.4103/jcrt.jcrt_1584_23
Quick Response Code:

ABSTRACT

Objective: Radiotherapy is an effective treatment for brain tumors, but it can lead to adverse side effects, particularly neurocognitive dysfunction. The hippocampus, a crucial structure for memory formation, is vulnerable to radiation-induced damage. To reduce the risk of adverse effects, the precise delineation of the hippocampus is necessary for radiation therapy planning. Automated hippocampal delineation using deep learning and mask regions with convolution neural networks (R-CNN) algorithm reduces the manual delineation time, ensures accuracy, and supports its implementation in radiation therapy. This study aimed to develop an automated method for hippocampal delineation and assess its feasibility for brain radiation treatment using deep learning and Mask R-CNN algorithm.

Materials and Methods: The study applied several pre-processing techniques, including thresholding, Canny edge detection, and keypoint detection, to enhance the input images of patient hippocampal scans. The processed images were then analyzed using the Mask R-CNN algorithm for automated hippocampal delineation. The Mask R-CNN algorithm was assessed using the following metrics: accuracy, recall, intersection over union (IoU), and mean average precision (mAP).

Results: The proposed network achieved a mAP of 96.2% and average sensitivity of 0.93, indicating high segmentation accuracy. Moreover, the recall was 0.87 and specificity was 0.96, indicating the high specificity of the method to segment the hippocampus.

Conclusions: The results of this study suggest that the developed automated method is highly sensitive and specific for delineating the hippocampus. This automated segmentation method may be used to complement the manual review of hippocampal scans during radiotherapy planning for brain tumors.

KEY WORDS: Artificial intelligence, auto-delineation, hippocampus, Mask R-CNN, radiotherapy

INTRODUCTION

Brain tumors—both primary and secondary—represent a serious public health issue. Primary brain tumors and brain metastases have been observed to occur more frequently recently. The dentate gyrus of the hippocampus, a region responsible for adult neurogenesis, has been identified as one of the primary brain sites susceptible to radiation injury.[1,2] Preclinical studies have suggested that radiation-induced loss of hippocampal stem cells and modifications to the structure and function of mature neurons may contribute to cognitive decline and other hippocampus-related side effects, including emotional alterations.[1,2] Radiation therapy has been a valuable treatment modality for primary and secondary brain tumors, providing patients with survival and quality of life benefits.[1,2] While whole-brain radiation therapy is an important treatment modality in brain metastasis management, it poses severe neurocognitive effects in patients.[3,4] These effects are especially concerning in children, who may experience long-term impacts on their neurocognitive development.

The accurate delineation of the hippocampus is crucial during radiation therapy planning to reduce the risk of radiation-induced adverse effects. However, manual hippocampus delineation is a time-consuming and challenging task in clinical practice owing to the region's tiny volume and diffuse boundaries. Therefore, this study aimed to develop an artificial intelligence (AI)-based

Cite this article as: Laud A, Talapatra K, Sankhe M, Gupte A, Shetty A, Bardeskar N, *et al*. Auto-delineation of the hippocampus using Mask R-CNN for radiation oncology: A cross-sectional observational study. J Can Res Ther 2024;20:1781-7.

automated system for the hippocampal region using deep learning segmentation techniques. This automated method for the delineation of the hippocampus was developed to evaluate the feasibility of hippocampal-sparing methods during brain radiation.

MATERIALS AND METHODS

General study details

This cross-sectional study included the data of patients without any brain abnormalities who underwent magnetic resonance imaging (MRI) at a tertiary care hospital from June 2022 to August 2022. The patient datasets included MRI scans, particularly of the hippocampal region, in the digital imaging and communications in medicine (DICOM) format. These datasets are used for evaluating and analyzing specific characteristics or conditions related to the brain for radiotherapy planning. Ethical approval was obtained from the institutional ethics committee (IEC) on June 6, 2022, with approval number BNH/1033/2022, and the requirement of informed consent was waived considering the collection of anonymized patient data. The study was conducted in accordance with the Declaration of Helsinki.

Participants

We included patients aged >18 years without any brain abnormalities who visited the hospital's radiology department for MRI. Those who were detected with brain anomalies were excluded from the study. All patient data were anonymized.

Objectives

Hippocampal radiation injury can lead to negative consequences later in life, particularly in neurocognitive domains connected to memory. The hippocampus is responsible for early changes in cognitive function following radiation side effects. This study aimed to develop an AI-based automated system using deep learning segmentation techniques that facilitate the automated analysis of the hippocampus and support the use of radiation therapy to treat brain cancers or brain metastases, thereby sparing the hippocampal region.

Study methodology

A. Extraction of image slices.

The ground truth data were first manually annotated by four authors with an average experience of 3 years. Any disagreements among these authors were resolved by a fifth author who had an average experience of 20 years. The patients underwent MRI of the brain on 3-Tesla GE Medical System MRI Machine (GE Healthcare, Chicago, IL). The morphological and anatomical assessment of the hippocampus was performed using the following scan protocol and sequence: SAGT1, SpGR, and Cube FLAIR CoRT2 (FOV, 25.6 mm^2; matrix, 256 × 256; NEX, 1; slice thickness, 2.2 mm). The dataset comprised a DICOM (.dcm) file that contained the contours of the hippocampal region. Every DICOM contour file has information embedded in an unstructured tree-like manner. It is important to get the correct sequence of slices of a DICOM image, especially when .dcm files for each slice might be arbitrarily ordered by name. The correct sequence is also very important for working directly with 3D voxels, for example, using 3D CNNs.[5] The DICOM files contained each MRI output slice along with a single file with the contour information for a specific MRI sequence. Different contour sequences were identified using dicom-contour, a Python library that converts DICOM images and contours into arrays for extracting image and mask voxels. The image slices were extracted in a sorted order using an index given by the referenced region of interest (ROI) number in the file itself. Supplementary Figure 1 displays an image slice.

B. Mask concatenation.

DICOM contouring consists of two masks, namely the left and right hippocampuses. These masks are concatenated to generate common masks for detection. Each mask is of 512 × 512 pixels. The first image in Figure 1. shows the left hippocampus contour extracted from the DICOM files, represented in the red green blue (RGB) format. The second image is the original medical image extracted from the DICOM files. The third image is the right hippocampus contour extracted from the DICOM files, represented in the RGB format. Finally, the fourth image is a concatenated image of the left and right hippocampus contours. This image was created by adding the left and right hippocampus contours using a weighted addition and then overlaying the resulting image on the original medical image. The visualization of hippocampal contours extracted from medical imaging data is useful in evaluating the accuracy of automated segmentation algorithms.[6] The resulting images were used to compare the performance of different segmentation algorithms as well as to identify the areas of improvement in the segmentation process.

C. Thresholding.

The grayscale images were implemented using binary thresholding. This analysis technique is a type of image segmentation method that isolates contours by converting grayscale into binary images by setting a threshold value. In medical image analysis, thresholding is a common image processing technique used to segment an image by separating the foreground from the background.[7] After loading the images, the left and right labels were concatenated to form a single image of the hippocampus by adding weights to blend images together to create a composite image with adjustable contrast. Then, a thresholding operation was applied to the original image using the threshold function with a threshold value of 70. The resulting threshold image is displayed in Figure 2.

$$dist(x,y) = \begin{cases} maxval & ifsrc(x,y) > thresh \\ 0 & otherwise \end{cases}$$

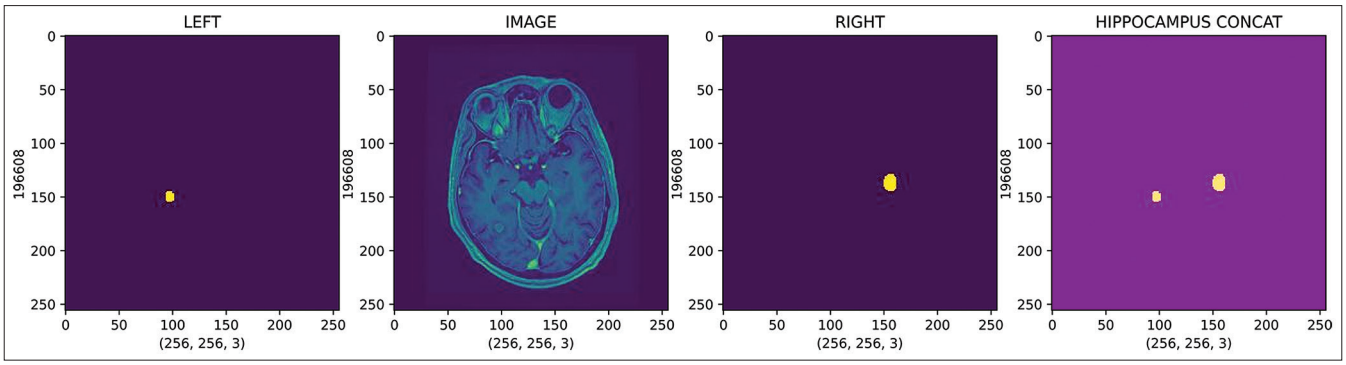

Figure 1: Concatenated mask

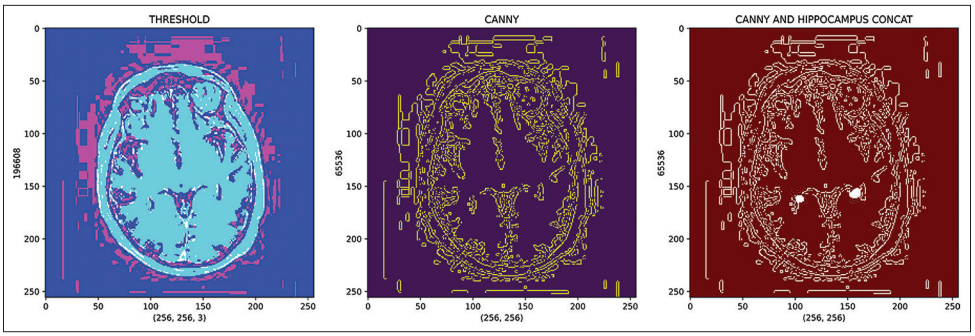

Figure 2: Results of thresholding and Canny edge detection

Eqn. (1). Thresholding.

D. Canny edge.

In hippocampus segmentation, the Canny edge detector is commonly used to extract the edges of the hippocampus region from brain MRI images. The hippocampus region can be easily distinguished from the surrounding brain tissues because it has a distinct shape and intensity.[8] Applying the Canny edge detector to the threshold image of the hippocampus helps obtain a binary image that highlights the edges of the hippocampus region. These edges can then be used to segment the hippocampus region from the surrounding brain tissues. The use of Canny edge detection can improve the accuracy of hippocampus segmentation by reducing the effect of noise and other artifacts in the MRI images. The Canny filter is a multistage edge detector that uses a filter based on the derivative of a Gaussian kernel to compute the intensity of the gradients. The Gaussian kernel reduces the effect of noise present in the image, as shown in Figure 2. The Canny edge reduces the noise and focuses on the ROI by excluding the outer brain tissues.

$$H_{ij} = \frac{1}{2\pi\sigma^2} exp\left(-\frac{(i-(k+1))^2 + (j-(k+1))^2}{2\sigma^2} \right); 1 \le i, j \le (2k+1)$$

Eqn. (2). Equation for Gaussian filter kernel of size (2k+1) *(2k+1) (for gradient calculation).

E. Keypoint detection.

Keypoint localization is performed using the scale-invariant feature transform (SIFT) algorithm by detecting and describing distinctive local features or keypoints in an image. The SIFT algorithm functions by first detecting potential keypoints in an image using a scale-space extrema detection approach. Then, the keypoints are refined using a process called keypoint localization, which aims to accurately locate the keypoints with subpixel precision.[4] After the keypoints are located as shown in Figure 3, their descriptors are computed using gradient orientation histograms. These descriptors are invariant to scale and rotation, making them highly distinctive and robust to image transformations.

The keypoints and their descriptors can be used for various computer vision tasks, such as image matching, object recognition, and scene reconstruction.[9] In the context of hippocampus research, this technique is used to analyze hippocampal images and identify specific features of interest (such as the dentate gyrus) or subfields. It is used for automated image analysis and classification of hippocampal images.

F. Building annotations.

Keypoints are converted into annotations, and the positions of key features in an image are stored as information in a JavaScript object notation (JSON) file. It contains information about each keypoint, including its position in the image,

its label, and any other relevant metadata. These data are used to train deep learning models to recognize and locate these hippocampus positions in testing images. Annotations typically include information about the locations of key features or objects in an image, such as the position of a landmark or boundaries of hippocampal tissues. This information is typically represented as a set of coordinates that define the location, shape, and size of the feature or tissue being annotated.

G. Model Implementation.

Mask regions with convolution neural networks (R-CNN) is a deep neural network designed to address segmentation challenges in the fields of machine learning and computer vision. The framework encompasses two main stages. Initially, it generates proposals concerning potential regions within the input image that may contain objects. Subsequently, it predicts the object's class, fine-tunes the bounding box, and generates a pixel-level mask for the object based on the proposals from the initial stage. Both stages are interconnected with a backbone structure, which is a deep neural network following a feature pyramid network-style architecture. The backbone comprises a bottom-up pathway, top-down pathway, and lateral connections. The bottom-up pathway, typically implemented using ConvNets such as ResNet or visual geometry group, is responsible for extracting features from the raw images. For our model, Inception ResNet was used. The network was trained using annotated MRI scans of the brain, with the hippocampus annotated as the target region.[10-14] The annotations are used to train the network to accurately localize and segment the hippocampus from the brain MRI scans. We proactively managed overfitting by incorporating dropout, weight decay, and validation-based early stopping. This resulted in enhanced generalization and a well-balanced model performance on both training and unseen data.

During inference, the proposed network takes an MRI scan as input and outputs a binary mask that represents the segmented hippocampus. This binary mask can be used for the analysis and study of the hippocampus. The methodology is summarized in Supplementary Figure 2.

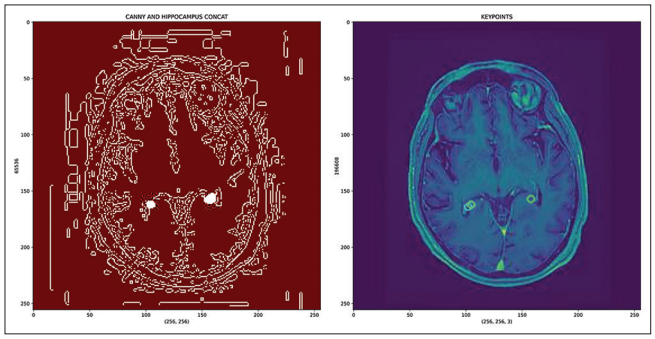

Figure 3: Keypoint detection

Statistical analysis

This was a cross-sectional preliminary study to evaluate whether AI can be used to auto-delineate the hippocampal regions for brain radiation planning. Considering that this was a pilot study, sample size calculation was not performed. The study AI algorithm was assessed using the metrics of accuracy, recall, intersection over union (IoU), mAP, and Dice coefficient along with specificity and sensitivity. All statistical analyses were performed using TensorFlow (version: 2.12.0; Google Brain, Mountain View, CA).

RESULTS

The Mask R-CNN model was implemented on a dataset of 25 patients who underwent MRI for non-brain-related illness and trained using stochastic gradient descent optimization with a learning rate of 0.008 and momentum of 0.9. We employed a batch size of 2 and trained the model for 15000 epochs. The training process involved minimizing the combined loss, including the classification loss, bounding box regression loss, and mask segmentation loss.

A. Evaluation metrics.

To evaluate the performance of the hippocampus segmentation, we employed several commonly used metrics, including accuracy, recall, IoU, and mAP.[12] These metrics provide a comprehensive assessment of the segmentation accuracy, including both shape and spatial localization.

The trained Mask R-CNN model achieved promising results for hippocampus segmentation on the testing set. The average mAP and recall scores were 0.962 and 0.87, respectively, indicating a high overlap between the predicted and ground truth masks as shown in Table 1. The Dice coefficient of the model implemented on the test set and validation set was 0.93, whereas the mAP of the validation set was 0.94. The model exhibited an average sensitivity of 0.93, demonstrating its ability to capture most of the hippocampal region, whereas the average specificity was 0.96, indicating the model's capability to accurately identify regions outside the hippocampus [Figure 4].

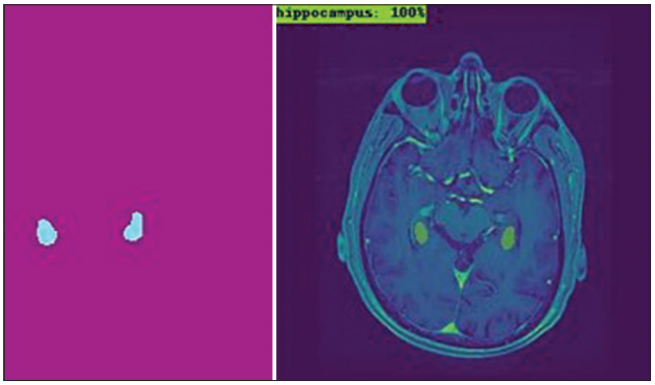

Figure 4: Result of segmentation (left: input mask (manually marked); right: generated mask by model)

Table 1: Results of mask R-CNN model

Property	Intersection over union	Area	Value (%)
Average precision (AP)	IoU=0.50:0.95	Area=all	0.962
Average precision (AP)	IoU=0.50	Area=all	0.986
Average precision (AP)	IoU=0.75	Area=all	0.984
Average precision (AP)	IoU=0.50:0.95	Area=small	-1.000
Average precision (AP)	IoU=0.50:0.95	Area=medium	-1.000
Average precision (AP)	IoU=0.50:0.95	Area=large	0.937
Average recall (AR)@1	IoU=0.50:0.95	Area=all	0.874
Average recall (AR)@10	IoU=0.50:0.95	Area=all	0.885
Average recall (AR)@100	IoU=0.50:0.95	Area=all	0.885
Average recall (AR)	IoU=0.50:0.95	Area=small	-1.000
Average recall (AR)	IoU=0.50:0.95	Area=medium	-1.000
Average recall (AR)	IoU=0.50:0.95	Area=large	0.885

B. Average precision (AP) metrics.

The evaluation results indicated high precision across a wide range of IoU thresholds (0.50 to 0.95) for all object sizes, with an overall value of 96.2%. This demonstrated the effectiveness of the model in accurately detecting objects. In particular, at a lower IoU threshold of 0.50, the precision remained high, as reflected by an AP value of 98.6%. Likewise, at a higher IoU threshold of 0.75, the precision remained consistent, with an AP value of 98.4%.

There were no ground truth annotations available for objects categorized as "small" or "medium" areas, resulting in the AP values of −1.000 for both categories. This implied that the evaluation was unable to assess the model's precision for these specific object sizes. By contrast, for objects categorized as "large," the model achieved a precision of 0.937 across a range of IoU thresholds (0.50 to 0.95). These evaluation metrics provided valuable insights into the model's performance in object detection, indicating high precision across different IoU thresholds and object sizes, with the exception of "small" and "medium" categories where ground truth annotations were unavailable. Moreover, the Mask R-CNN approach demonstrated a substantial reduction in manual correction time—up to 40% approximately when compared to manual delineation alone. Thus, these findings demonstrate the model's capability to accurately detect objects, particularly larger ones, and highlight areas for further improvement in terms of object size-specific performance evaluation.

C. Average recall (AR) metrics.

The recall evaluation results demonstrated the model's performance for object detection. The model achieved a recall of 0.874 at AR@1 and 0.885 at AR@10 for all object sizes, considering the IoU thresholds from 0.50 to 0.95. The overall recall, measured by AR@100, was 0.885, indicating consistent object detection across IoU thresholds. However, no ground truth annotations were available for "small" and "medium" objects, preventing the evaluation of recall performance. For "large" objects, the model achieved a recall of 0.885 across all IoU thresholds. In summary, the evaluation metrics showed the model's ability to capture a significant number of objects, especially larger ones, while highlighting the need for ground truth annotations for smaller and medium-sized objects, as shown in Table 1.

DISCUSSION

The manual delineation of the hippocampus is time-consuming and challenging in clinical practice owing to its small volume and diffuse boundaries. This study aimed to investigate the use of deep learning techniques, specifically the Mask R-CNN architecture, for the automatic delineation of the hippocampus. By leveraging AI and deep learning algorithms, a robust and efficient tool was developed to autosegment the hippocampus from brain MRI images. The study addressed the need for the precise delineation of the hippocampus to facilitate advanced treatment planning techniques that aim to spare the hippocampus during radiation therapy, thereby mitigating radiation-induced neurocognitive side effects. The study aimed to assess the accuracy and efficiency of the automated hippocampus segmentation method. The results of the automated segmentation were compared using the Mask R-CNN implementation, which helped build accurate masks. The proposed network achieved a high mAP of 96.2%, indicating excellent segmentation accuracy.

A previous study investigated the following methods: fully convolution neural network (FCNN), conditional random field (CRF), and three-dimensional conditional random field (3D-CRF).[15] FCNN + CRF + post-process and FCNN + 3D-CRF + post-process achieved the highest Dice coefficients, with values of 0.87, indicating a strong overlap between the predicted and ground truth segmentation masks. The method of FCNN + post-process also achieved a high Dice coefficient of 0.81, indicating good segmentation accuracy. The methods FCNN + 3D-CRF + post-process and FCNN + 3D-CRF achieved the highest positive predictive value (PPV values), with values of 0.78 and 0.73, respectively. This suggests that these methods had a lower rate of false-positive predictions. The method of Leaderboard FCNNs achieved the highest sensitivity value of 0.96, indicating a high rate of true-positive prediction. Other methods, such as FCNN + CRF and FCNN + CRF + post-process.

Also achieved relatively high sensitivity values of 0.85 and 0.84, respectively.[15] This study implementing Mask R-CNN exhibited an average sensitivity of 0.93 and average specificity of 0.96. The Dice coefficient result for the test set and validation set was 0.93. A Dice coefficient of 0.93 signifies that approximately 93% of the segmented regions in the predicted masks aligned with the corresponding regions in the ground truth masks. Thus, our Mask R-CNN model outperformed the previous study's FCNN-based methods,[15] achieving a Dice coefficient of 0.93 versus their best of 0.87. The Mask R-CNN model achieved high precision and recall for objects and outperformed the aforementioned models across various IoU thresholds and area categories, except for the "small" and "medium" areas where no ground truth annotations were available. These results demonstrated the effectiveness of the object detection system in accurately localizing and classifying objects, particularly for larger sizes. The model's high sensitivity and specificity with high segmentation performance support its ability to correctly identify the hippocampal region while minimizing false positives and false negatives. The high mAP and recall scores indicated a close match between the predicted and ground truth masks, highlighting the accuracy of the segmentation. We mitigated class imbalance using focal loss and data augmentation, enhancing our model's ability to accurately segment the smaller hippocampus class. These strategies contributed to achieving impressive segmentation results despite the class imbalance challenge. In addition, we extended training steps and upscaled image dimensions from 256 × 256 to 512 × 512. This not only improved overall segmentation performance but also contributed to reducing class imbalance effects. The higher resolution allowed the model to capture finer details of the smaller class, leading to more balanced and accurate segmentation results. Further, we carefully considered the practical integration of the Mask R-CNN architecture, especially in the context of our target audience, clinicians. Thus, we explored model optimization techniques such as model quantization and pruning, thereby significantly reducing inference time and memory consumption. These efforts ensured the feasibility of real-world deployment, making our approach valuable and applicable in clinical settings without compromising its segmentation accuracy.

During the training process of the deep learning model, a learning rate schedule was incorporated to optimize the model's performance. The learning rate gradually increased from 0 to 0.08 during the initial phase, allowing the model to explore a broader range of learning rates and adapt quickly. It then remained constant at 0.08, enabling the model to fine-tune its parameters and converge toward an optimal solution. The curve exhibited a gradual increase in mAP as the model underwent training as shown in Supplementary Figure 3. This upward trend demonstrated the model's ability to learn and improve its performance over successive epochs.

The learning rate of the developed model was subjected to training using the patient image datasets. The mAP values were monitored closely during the training process, and after the 12000th epoch, the average mAP was 0.962 [Figure 5]. Some challenges and limitations were observed during the segmentation process. In cases where there were certain imaging artifacts, such as intensity variations and partial volume effects, the model exhibited decreased performance. Improvements in pre-processing techniques and data augmentation strategies could potentially mitigate these limitations.

The key limitations of the study include manual annotation dependency as the performance of Mask R-CNN highly relies on the quality and accuracy of the annotated ground truth data used for training. The manual annotation of hippocampus regions is susceptible to human errors and interobserver variability. Any inaccuracies or inconsistencies in the ground truth annotations can propagate to the model's predictions and limit its overall performance. However, they were minimized as far as possible. Mask R-CNN is a computationally demanding model owing to its complex architecture, which includes a region proposal network (RPN), backbone network (e.g., ResNet), and additional mask prediction layers. This complexity can lead to increased inference time and memory requirements, making it less suitable for real-time or resource-constrained applications. In many medical imaging tasks, including hippocampus segmentation, the class distribution can be imbalanced, with the target class (hippocampus) being significantly smaller in comparison with the background class. This class imbalance can affect the model's ability to accurately segment the hippocampus and may require additional techniques, such as data augmentation, class weighting, or specialized loss functions, to address the issue. Mask R-CNN may struggle to accurately delineate the precise boundaries of the hippocampus, particularly in cases where there are ambiguities or indistinct boundaries in the imaging data. The model's segmentation masks may exhibit jagged edges or leak into neighboring structures, reducing the accuracy of the segmentation results. Finally, the study included scans

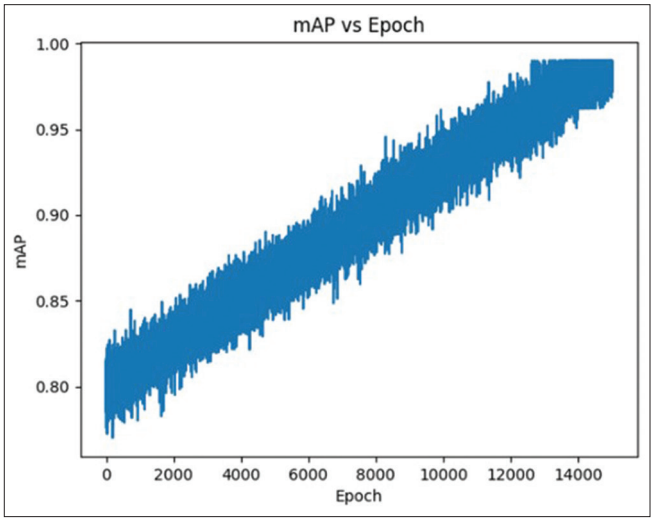

Figure 5: mAP/Epoch

performed using only one MRI machine and analyzed only healthy adult individual data. The credibility of the model's performance would indeed be increased by comparing data from patients with brain tumors. Hence, considering the small dataset and positive results of this study, we hope to replicate the study using a large dataset of healthy individuals and patients with brain tumor with scans performed on different MRI systems and compare the performance of Mask R-CNN with other architectural models to validate the model's performance.

CONCLUSION

The developed tool demonstrated robustness and efficiency in segmenting the hippocampus from brain MRI images, addressing the need for precise segmentation in radiation therapy to minimize neurocognitive side effects. The Mask R-CNN implementation achieved an impressive mAP of 96.2%, surpassing previous methods in terms of precision, recall, and sensitivity, particularly for larger objects. The model accurately localized and classified objects, providing precise hippocampus segmentation while minimizing false positives and false negatives. However, the presence of imaging artifacts, dependency on manual annotation, class imbalance, and difficulty in delineating precise boundaries affected the model's performance. This study demonstrated the effectiveness of Mask R-CNN in automating hippocampus segmentation. Future research should focus on addressing the identified limitations and exploring techniques to enhance the model's accuracy and efficiency in real-world clinical settings.

Authors contribution

AL, KT, and MS conceived or designed the work. AL, AG, AS, AR, SB, PT, and AS collected the data. AL, AG, AS, AR, SB, PT, and AS analyzed and interpreted the data. AL, NB, and PK drafted the manuscript. KT, DP, and MS made critical revision of the article. All authors made final approval of the version to be published. KT agreed to be accountable for all aspects of the work.

Data sharing statement

Individual de-identified participant data will be made available on reasonable request, from Dr. Kaustav Talapatra (kaustee@gmail.com), until 10 years after publication. In addition, the study protocol including statistical analysis plan is already available in the main text.

Financial support and sponsorship

Nil .

Conflicts of interest

There is no conflicts of interest.

REFERENCES

1. Redmond KJ, Milano MT, Kim MM, Trifiletti DM, Soltys SG, Hattangadi-Gluth JA. Reducing radiation-induced cognitive toxicity: Sparing the hippocampus and beyond. Int J Radiat Oncol Biol Phys 2021;109:1131-6.
2. Son Y, Yang M, Wang H, Moon C. Hippocampal dysfunctions caused by cranial irradiation: A review of the experimental evidence. Brain Behav Immun 2015;45:287-96.
3. Feng CH, Cornell M, Moore KL, Karunamuni R, Seibert TM. Automated contouring and planning pipeline for hippocampal-avoidant whole-brain radiotherapy. Radiat Oncol 2020;15:1-6.
4. Qiu Q, Yang Z, Wu S, Qian D, Wei J, Gong G, *et al*. Automatic segmentation of hippocampus in hippocampal sparing whole brain radiotherapy: A multitask edge-aware learning. Med Phys 2021;48:1771-80.
5. Zhou T, Fu H, Chen G, Shen J, Shao L. Hi-net: Hybrid-fusion network for multi-modal MR image synthesis. IEEE Trans Med Imaging 2020;39:2772-81.
6. Thyreau B, Sato K, Fukuda H, Taki Y. Segmentation of the hippocampus by transferring algorithmic knowledge for large cohort processing. Med Image Anal 2018;43:214-28.
7. Suzuki H, Toriwaki J. Automatic segmentation of head MRI images by knowledge guided thresholding. Comput Med Imaging Graph 1991;15:233-40.
8. Wang M, Zheng S, Li X, Qin X. A new image denoising method based on gaussian filter. 2014 international conference on information science, electronics and electrical engineering, Sapporo, Japan 2014;26:163-7.
9. Li S, Chen S, Li H, Ruan G, Ren S, Zhang T, *et al*. Anatomical point-of-interest detection in head MRI using multipoint feature descriptor. IEEE Access 2020;8:173239-49. “”
10. He K, Gkioxari G, Dollár P, Girshick R, “Mask R-CNN,” 2017 IEEE International Conference on Computer Vision (ICCV), Venice, Italy, 2017; pp. 2980-2988.
11. Ataloglou D, Dimou A, Zarpalas D, Daras P. Fast and precise hippocampus segmentation through deep convolutional neural network ensembles and transfer learning. Neuroinformatics 2019;17:563-82.
12. Carmo D, Silva B, ’Yasuda C, Rittner L, Lotufo R. Hippocampus segmentation on epilepsy and Alzheimer’s disease studies with multiple convolutional neural networks. Heliyon 2021;7:e06226.
13. Pan K, Zhao L, Gu S, Tang Y, Wang J, Yu W, *et al*. Deep learning-based automatic delineation of the hippocampus by MRI: Geometric and dosimetric evaluation. Radiat Oncol 2021;16:12.
14. Marins T, Rodrigues EC, Bortolini T, Melo B, Moll J, Tovar-Moll F. Structural and functional connectivity changes in response to short-term neurofeedback training with motor imagery. Neuroimage 2019;194:283-90.
15. Zhao X, Wu Y, Song G, Li Z, Zhang Y, Fan Y. A deep learning model integrating FCNNs and CRFs for brain tumor segmentation. Med Image Anal 2018;43:98-111.

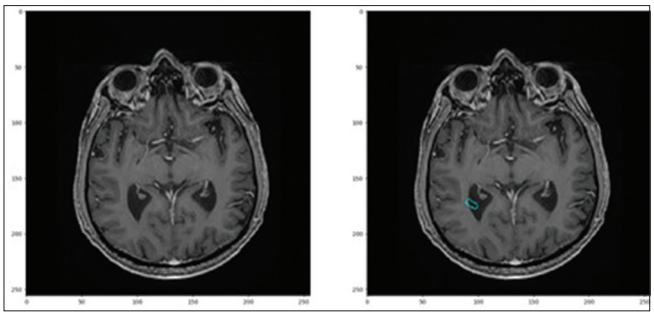

Supplementary Figure 1: Extraction of slice

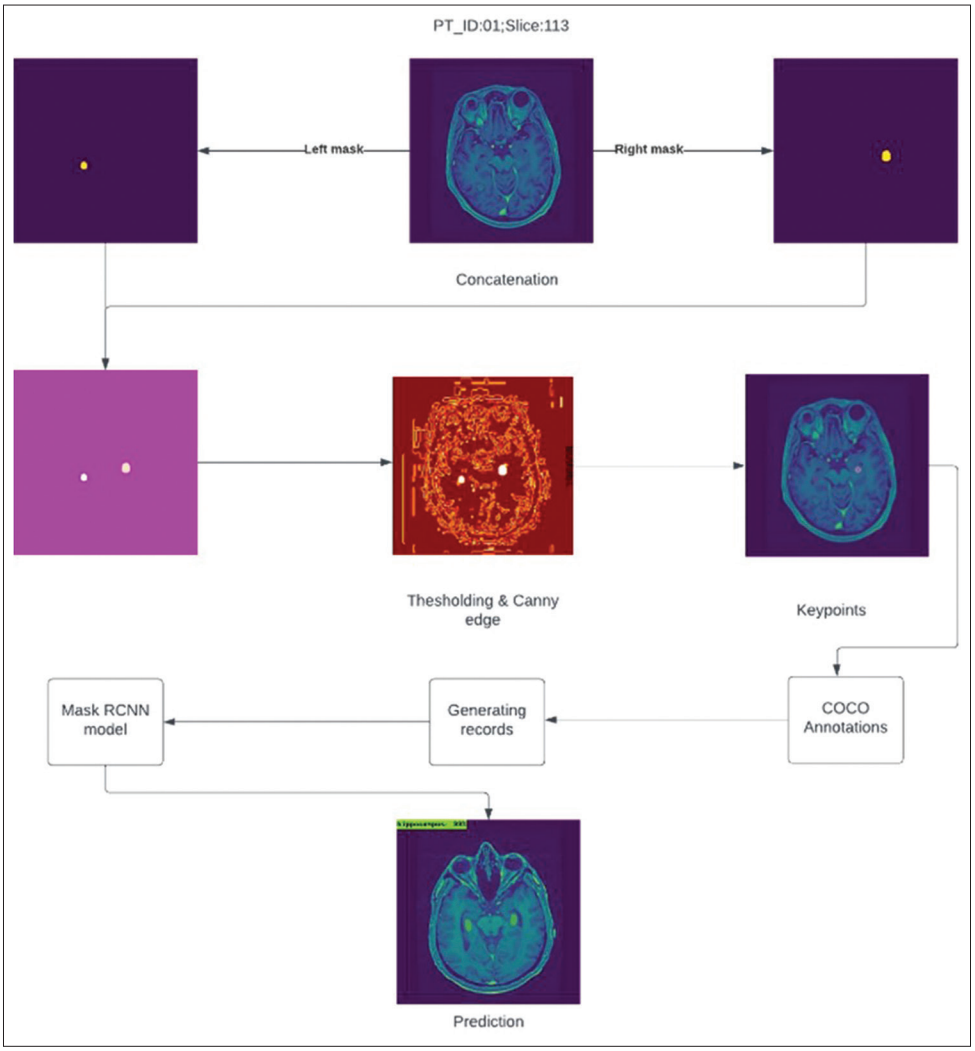

Supplementary Figure 2: Flowchart of study methodology

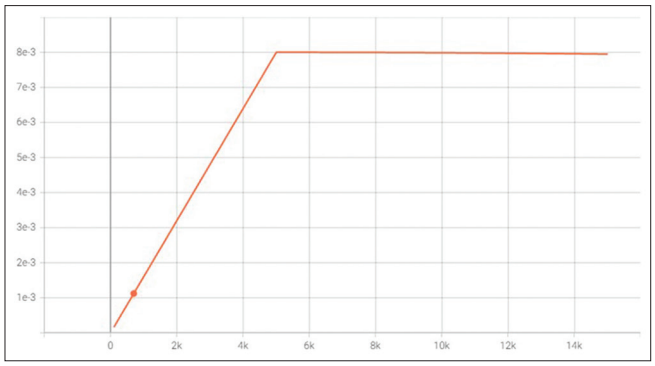

Supplementary Figure 3: Learning rate/Epoch